# *A comprehensive study about alongshore wave energy flux in the coast of Buenos Aires, Argentina*

**Emilio R. Echevarría, Walter C. Dragani & Stefania Wörner**

**Journal of Coastal Conservation**
Planning and Management

ISSN 1400-0350

J Coast Conserv
DOI 10.1007/s11852-018-0673-2

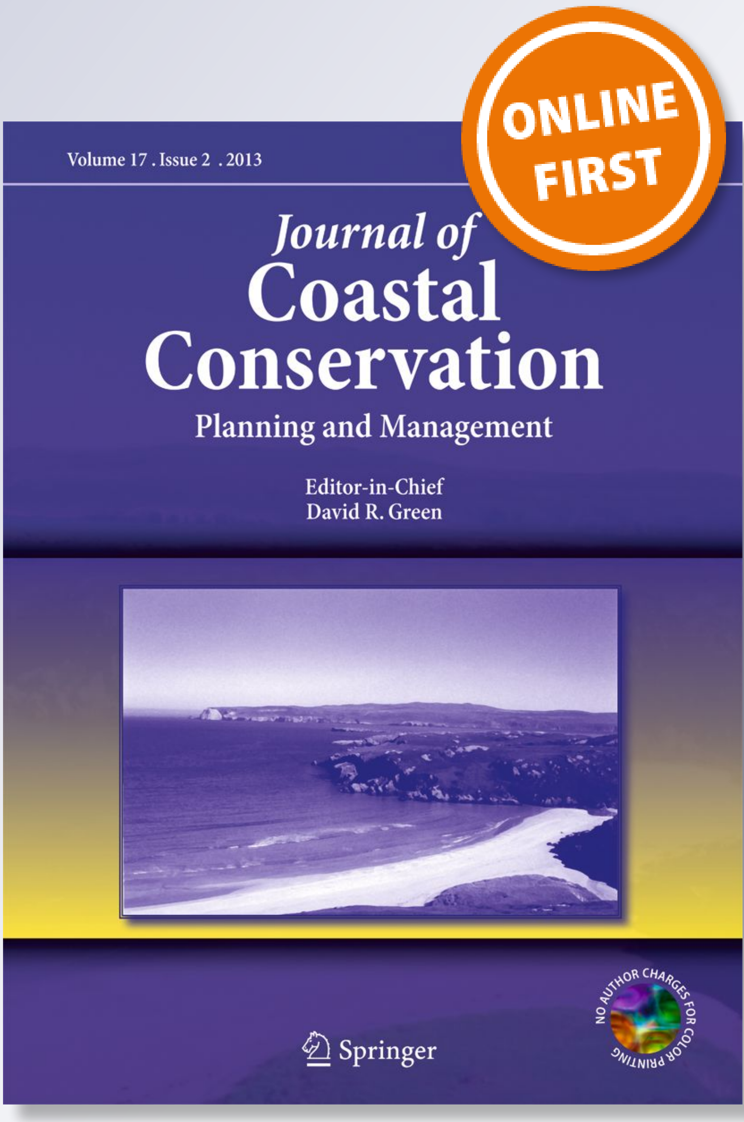


Springer

Journal of Coastal Conservation
https://doi.org/10.1007/s11852-018-0673-2

# A comprehensive study about alongshore wave energy flux in the coast of Buenos Aires, Argentina

Emilio R. Echevarría[1,2,3] • Walter C. Dragani[1,2,3] • Stefania Wörner[1,2,3]

Received: 6 September 2017 / Revised: 24 August 2018 / Accepted: 26 November 2018



## Abstract

Alongshore wave energy flux (*Pl)* was analysed for the coast of Buenos Aires, Argentina. *Pl* is frequently used to estimate the alongshore sediment transport rate. *Pl* was estimated from simulated offshore wave parameters obtained from a validated regional SWAN model forced by NCEP/NCAR I, NCEP/DOE II, ERA-Interim and JRA-25 global reanalysis for the year 2005. It was obtained that *Pl* flows eastwards/northeastwards and increases irregularly from Bahía Blanca to Mar del Plata. Negative and positive space imbalances in *Pl* along the coast could explain the natural erosive and constructive processes detected between Mar del Plata and Punta Médanos. High inter-annual variability was noted in *Pl* data series computed from simulated wave parameters using SWAN model forced by NCEP/NCAR I for the period 1980–2012. Anomalous *Pl* values were detected in 1983, 1993 and 1998 which are in agreement with reported ENSO events. Concluding, the applied methodology seems to constitute a very reasonable alternative to study the space and time variability of *Pl* at the Buenos Aires coast, between Bahía Blanca and Punta Médanos.


**Keywords** SWAN model · Simulated wave parameters · Atmospheric global reanalysis · Inter-annual variability · Erosion · Buenos Aires

## Introduction

The coast of the Buenos Aires province, located between 36°S and 39°S (Fig. 1), is constituted by sandy beaches, with seaside resorts which are crowded with tourists in the summer, and represents a very important economic and natural area (Juárez and Mantobani 2006; Marcomini and López 2006). The mean wave height along the coast slightly increases southwards and ranges from 1 to 1.5 m (Lanfredi et al. 1992). The mean wave direction is predominantly westwards, except at the southernmost part of the region where propagation is in general northwestwards (Dragani et al. 2010). Highest wind waves propagate mainly northwards during severe conditions or storms (Dragani et al. 2013a). The tide regime is mixed, predominantly semidiurnal and the tidal range also increases southwards from Punta Rasa (0.80 m) to Monte Hermoso (2.44 m) (Balay 1955; SHN 2017). Evident and progressive coastal changes produced by erosion is causing private capital losses and risks in nature and anthropologic reserves (Merlotto et al. 2013; Rojas et al. 2014). The area located approximately between Pehuén-Co and Monte Hermoso was established as a Geological, Paleontological and Archaeological Reserve and will be declared a World Heritage by UNESCO (*http://whc.unesco.org/en/tentativelists/5851/*). At the same time, this in particular constitutes a unique worldwide system due to the existence of anthropological and paleontological footprints (Bayón and Politis 1998).

Even though the Buenos Aires sandy beaches have touristic, economic and cultural importance, no environmental management action is being implemented to enhance or, at least to conserve, their resources. Likely, one reason of this inaction could be due to the lack of scientific environmental studies which allow understanding this complex coastal system. For instance, a fundamental quantity to be taken into account in the coastal environmental management is the annual rate of

✉ Walter C. Dragani
dragani@hidro.gov.ar

1 Servicio de Hidrografía Naval, Av. Montes de Oca 2124 (C1270ABV), Buenos Aires, Argentina

2 Consejo Nacional de Investigaciones Científicas y Técnicas (CONICET), Godoy Cruz 2290 (C1425FQB), Buenos Aires, Argentina

3 Departamento de Ciencias de la Atmósfera y los Océanos, Universidad de Buenos Aires, (C1428EGA), Buenos Aires, Argentina

Published online: 05 December 2018

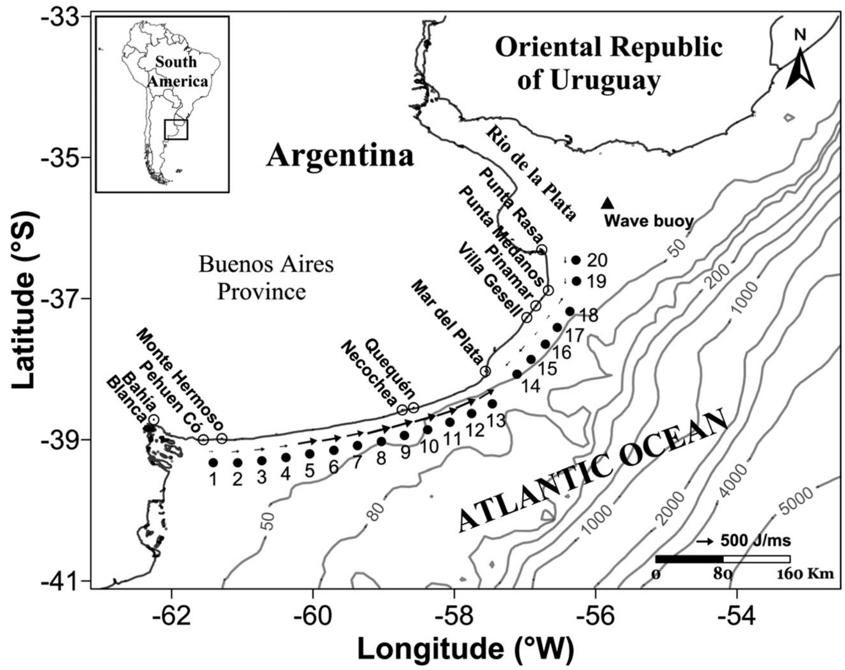


Fig. 1 Buenos Aires Province coast (Argentina) and its locations, in the Southwestern Atlantic Ocean. Numbers indicate the position where simulated wave parameters were carried out. Black triangle indicates the position of the wave gauge located at the outer Río de la Plata. Averaged annual net *Pl* (black arrows) computed from wave parameters simulated with SWAN model forced by NCEP/NCAR I reanalysis (period: 1980–2012) is also presented

alongshore sediment transport. The Coastal Engineering Research Center (CERC 1984) recommends simple methods to estimate this rate for a particular location. Nevertheless, if the alongshore sediment transport rate is required for an extended area (of several hundreds of kilometers long, such as the coast of Buenos Aires) the most convenient technique to estimate it could be the well known "energy flux method" (Galvin and Schweppe 1980). Alongshore energy flux can be computed from wave parameters obtained from a validated regional numerical model (see, for example, Verón and Bértola 2014). Very few scientific antecedents about the application of the energy flux method are available for the Buenos Aires coast. Simultaneous wave measurements, dredge, and bathymetric records were used by Caviglia et al. (1991) to calculate the dimensionless coefficient (*K*) between the sediment transport rate (*Q*) and the wave energy flux parallel to the coast (*Pl*). A northward net sediment transport of 3.9 $10^5$ $m^3$ $yr.^{-1}$ was obtained for Mar del Plata by Caviglia et al. (1991). Dragani et al. (2013b) used visual observations of breaker wave height and direction gathered at the surf zone in Pinamar (1989–2007) to estimate *Pl*. Northward net *Pl* and a weak negative long term trend were found. Recently, Perez et al. (2017) studied the variability and trends of *Pl* between Bahía Blanca and Mar del Plata. *Pl* was computed from wave parameters simulated with SWAN model, driven by NCEP/NCAR I reanalysis. *Pl* obtained were predominantly eastwards on the southern coast of Buenos Aires.

The assessment of *Q* would seem to be a particular subject for the marine geology or coastal oceanography. Several studies in Buenos Aires coast assigned the sediment transport mostly to the frequency and intensity of storms coming from the south (see, for instance, Fiore et al. 2009; Isla 2015). Nevertheless, *Q* is usually estimated by mean of *Pl* and, this last, calculated using wave heights and directions, which are directly dependent from the wind field and sediment availability. Consequently, one significant portion of the energy required for the alongshore sediment transport, the coastal erosion and many of the littoral processes is provided by the atmosphere, through the wind-wave generation. The main aim of this work is to present a comprehensive study of *Pl* along the Buenos Aires coast, between Bahía Blanca and Punta Rasa. Spatial and temporal variability of *Pl* (period: 1980–2012) is presented in this work. *Pl* was computed from simulated offshore (deep water) wave parameters, obtained from a validated regional SWAN model driven by NCEP/NCAR I global reanalysis. In addition, the performance of four different atmospheric databases (NCEP/NCAR I, NCEP/DOE II, ERA-Interim and JRA-25) implemented as forcing of SWAN model for computing *Pl* along the Buenos Aires coast is discussed in the present paper.

## Material and methods

The wave energy flux parallel to the coast (*Pl*) was computed along the Buenos Aires coast from modeled wind waves parameters obtained from SWAN model. SWAN model was forced by NCEP/NCAR I for the period 1980–2012 and validated with satellite wave heights obtained from the Globwave Project (Quefeffeulou and Croizé-Fillon 2013) and observed wave parameters gathered at the outer Río de la Plata (35°40'S and 55°50'W, Fig. 1).

### SWAN model: Architecture and implementation

SWAN is a spectral wave model that provides real estimations of wave parameters in coastal regions (Booij et al. 1999). For this region, the computational domain spans a range of latitudes between 29.747°S and 42.203°S, and a range of longitudes from 40.405°W to 65.418 °W. It provides gridded data with a spatial resolution of 22.7 × 20.0 km, resulting in 70 × 100 grid points, and a temporal resolution of 6 h. The bathymetry data for the SWAN model was obtained combining a depth dataset with 1′ × 1′ resolution taken from GEBCO charts (2003) and digitized nautical charts (SHN 1986, 1992, 1999a, b). These data were interpolated to the model grid by applying the method of inverse distance to the second power.

Surface wind data from NCEP/NCAR Reanalysis I were used to drive the simulation. The NCEP/NCAR I is a project between the National Center for Environmental Prediction (NCEP) and the National Center for Atmospheric Research (NCAR), which is available since 1948. It has a spatial resolution of 1.875° of longitude and 1.905° of latitude. NCEP/NCAR I reanalysis has been successfully utilized as forcing in several numerical regional studies in the area (see, for instance, Codignotto et al. 2012; Dragani et al. 2010; Simionato et al. 2005; Simionato et al. 2006a, b, 2007). A discussion about the quality of NCEP/NCAR I over the Southern Hemisphere can be found in Simmonds and Keay (2000). A complete description of this reanalysis and its dataset can be found in Kalnay et al. (1996). More details about the architecture, implementation, and validation (using in situ data) of SWAN model on the northern coast of Buenos Aires can be found in Dragani et al. (2008) and Martin et al. (2012). In addition, Perez et al. (2017) validated numerical simulations using satellite wave heights in the southern coast of Buenos Aires. Altimeter database obtained from the Globwave Project (Quefeffeulou and Croizé-Fillon 2013) consists on calibrated wave heights from eight missions: ERS-1, ERS-2, TOPEX-Poseidon, GEOSAT Follow-ON (GFO), Jason-1, Jason-2, ENVISAT and CryoSat, covering the 1991–2012 period. Computed mean bias, scatter index and correlation index were 0.04 m, 0.37 and 0.61, respectively.

### Estimation of the wave energy flux parallel to the coast (*Pl*)

The wave energy flux parallel to the coast (*Pl*) can be computed (Galvin and Schweppe 1980) as:

$$Pl = 0.05\rho g^{3/2} {H_{S0}}^{5/2} cos(\theta_0)^{1/4} sin(2\theta_0) \quad (1)$$

where $\rho$ is the sea water density (considered equal to 1030 kg m$^{-3}$), $g$ is the acceleration due to gravity, $H_{S0}$ the significant wave height and $\theta_0$ the wave direction, both parameters corresponding to deep waters. $\theta_0$ was transformed to give the angle between the wave crest and the shoreline. The coast of the study region is about 600 km long, and considering its general orientation can be divided in three different sectors: (i) from Bahía Blanca to Mar del Plata, with a predominant WSW-ENE orientation, (ii) from Mar del Plata to Punta Médanos, with a SSW-NNE orientation and (iii) from Punta Médanos to Punta Rasa, where the coast is practically oriented in the S-N direction. The predominant orientation of the shoreline was estimated from Landsat images (Data SIO, NOAA, U.S. Navy, NGA, GEBCO, source: Google Earth, 2017). Values of $\theta_0$ equal to zero correspond to normal incidence of waves and, consequently, *Pl* is equal to zero. *Pl* can only flow in two possible directions depending on the sign of the instantaneous value of $\theta_0$: right ward (positive) or leftward (negative), respect to an observer located on the coast and looking to the sea. The sediment transport rate ($Q$) can be estimated by means of the product between *Pl* and a dimensionless and empirical constant ($K$) (CERC 1984; U.S. Army Corps of Engineers 2017).

## Results

Space and time variability of *Pl* along the Buenos Aires coast were computed using wave parameters ($H_{S0}$ and $\theta_0$) obtained from SWAN model forced with NCEP/NCAR I for the period 1980–2012. Computed *Pl* is directly dependent on simulated $H_{S0}$ and $\theta_0$ but, both wave parameters are also clearly dependent on the implemented atmospheric forcing. Therefore, three additional global reanalysis were also used for driving SWAN model (NCEP/DOE II, ERA-Interim and JRA-25). Resulting alongshore energy fluxes were compared with *Pl* estimated from directional wave parameters gathered at the mouth of the Río de la Plata for 2005.

### Space and Time Variability of *Pl* along the Buenos Aires coast

Twenty points located 30 km off-shore and disposed of every 30 km along the coast were defined to evaluate *Pl* (Fig. 1). The location labeled as 1 is the south-westernmost one and the point labeled as 20 is the northernmost one. Temporal mean values and directions of *Pl* (period: 1980–2012) for locations labeled from 1 to 20 are presented in Figs. 2 and 1, respectively. Negative *Pl* indicates wave energy flux flowing predominantly east-northeast-wards, north-northeastwards or northwards, depending on the sector of the coast of Buenos Aires. Low values of mean *Pl* can be seen at the south-westernmost sector of the study region (Fig. 1, points 1 to 4). *Pl* gradually increases eastwards and reaches the highest value at the point 8, located 40 km south of Necochea, then *Pl* slightly decreases towards Mar del Plata (Fig. 1). It is important to remark that the mean *Pl* flows predominantly east-northeast wards between Bahía

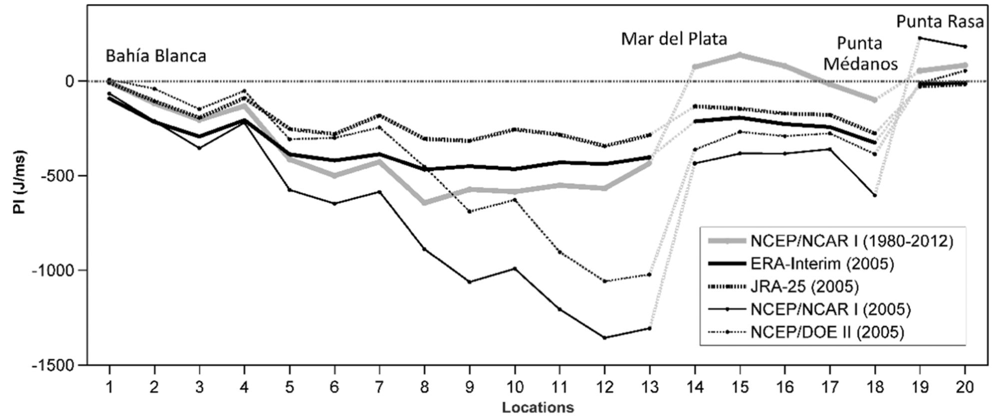


**Fig. 2** Averaged annual net *Pl* (period: 1980–2012) for locations 1 to 20, computed with simulated wave parameters from SWAN model forced by NCEP/NCAR I reanalysis, and net *Pl* (2005) computed with SWAN model forced with NCEP/NCAR I, NCEP/DOE II, JRA-25 and ERA-Interim reanalysis. Negative values correspond to eastward/northward *Pl*

Blanca and Mar del Plata. *Pl* becomes weak between Mar del Plata and Punta Médanos, from point 14 to 18. Mean directions of *Pl* are south-southwestwards at points 14, 15 and 16, and north-northeastwards at points 17 and 18. Finally, *Pl* directions are southwards at the northernmost part of the study area (points 19 and 20).

The interannual variability of *Pl* (period: 1980–2012) was also analyzed. Results obtained in this work revealed that the interannual variability of *Pl* presents distinctive features at each one of the three defined sectors of the Buenos Aires province coast: between Bahía Blanca and Mar del Plata, Mar del Plata and Punta Médanos, and Punta Médanos and Punta Rasa. Consequently, one particular location for each sector of the coast was selected for the analysis (points 6, 16 and 20). Annual mean values of *Pl* for each sector of the coast are presented in Fig. 3. Data series of *Pl* present a noticeable annual variation. *Pl* is mostly negative (east-northeastwards) - except for 1983, 1993, 1998 and 2001 -with values ranged from −1500 to 500 $Jm^{-1}s^{-1}$ between Bahía Blanca and Mar del Plata (location 6, Fig. 3.a). On the contrary, mean annual *Pl* are frequently lower, with values ranged between ±200 $Jm^{-1}$ $s^{-1}$ (16 of 33 years), or positive (south-southwestwards) with values lower than 1000 $Jm^{-1}$ $s^{-1}$ (11 of 33 years) between Mar del Plata and Punta Médanos (location 16, Fig. 3.b). Minimum *Pl*, around −1500 $Jm^{-1}$ $s^{-1}$ is detected for 1993. Finally, mean annual *Pl* are usually low, with values ranged between ±200 $Jm^{-1}$ $s^{-1}$ (for 23 of 33 years), positive (southwards) with values lower than +400 $Jm^{-1}$ $s^{-1}$(6 of 33 years) or negative (northwards) with values around −500 $Jm^{-1}$ $s^{-1}$ (4 of 33 years) between Punta Médanos and Punta Rasa (location 20, Fig. 3.c). Mean *Pl* computed between Punta Médanos and Punta Rasa is 82 $Jm^{-1}$ $s^{-1}$ (period: 1980–2012).

**Fig. 3** Annual net *Pl* data series (period 1980–2012), computed from wave parameters simulated with SWAN model forced by NCEP/NCAR I reanalysis, corresponding to (**a**) locations 6, (**b**) 16 and (**c**) 20. Thin lines delimit the interval ± 200 $Jm^{-1}$ $s^{-1}$ in (**b**) and (**c**)

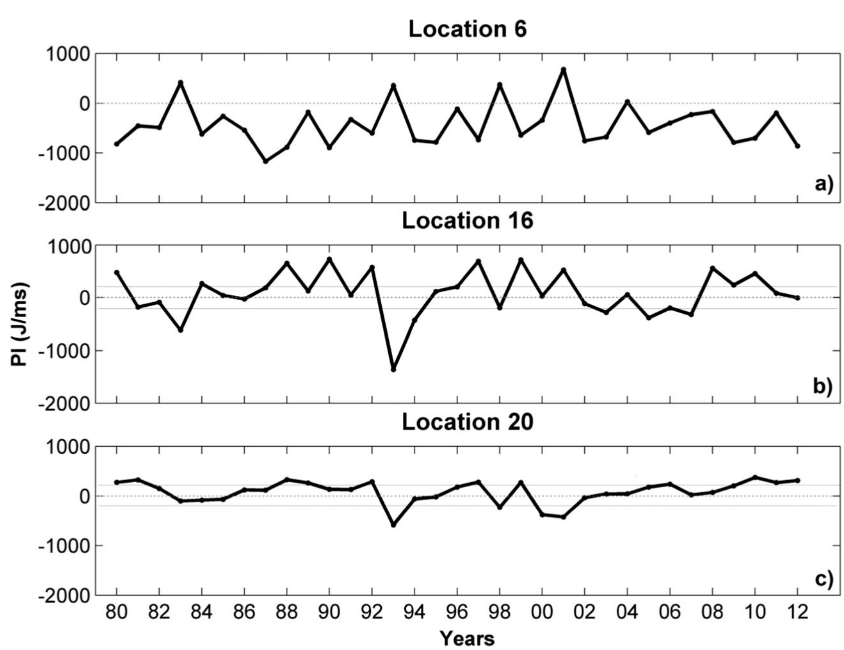

## *Pl* computed from wave observations at the northern coast of Buenos Aires

There are no long-term wave data series gathered in the study region between locations 1 and 20. The single long-term wave directional data series in the region was obtained from a Datawell Waverider buoy (Datawell 1997) moored at 16 m depth, approximately 115 km northeastwards from location 20 (35°40'S and 55°50'W, Fig. 1). The instrument was configured to take sea level records of 20 min each, with a 0.5 s sampling interval and every 160 min. Time series have several gaps, one of them longer than 1 year, three of them 8 months long, and six others of various durations. The data acquisition undertaken in the year 2005 was almost complete and, consequently, it was selected for this study. In addition, it is important to remark that SWAN model in the northern Buenos Aires coast was validated using these data series (Dragani et al. 2008).

The bottom topography at the southern outer Río de la Plata, that is, the region where point 20 and the buoy were located, is quite smooth and does not show remarkable bathymetry forms (SHN 1999b). In addition, point 20 and the buoy location are similarly exposed to the wave climate. Waves propagate 43.7% from the SE, 24.9% from the E and 14.4% from the S (Dragani et al. 2013a). Then, *Pl* at the point 20 (15 m depth) can be reasonably estimated from wave parameters recorded by the buoy. The mean annual *Pl* computed at the point 20 from observed wave parameters for 2005 was −926 $Jm^{-1}$ $s^{-1}$, which corresponds to a net northward flux. Instantaneous values of *Pl,* computed from observed wave parameters for the year 2005, is presented in Fig. 4. It can be clearly seen that *Pl* is predominantly negative (northwards). Two significant negative peaks can be appreciated in Fig. 4 which are associated with two severe events recorded in 08/24/2005 (wave height: 4.89 m and wave direction: 180°) and 01/31/2005 (4.71 m, 152°) during the presence of an extratropical cyclone located on the continental shelf adjacent to the Río de la Plata estuary (Dragani et al. 2013a). On the other hand, the mean annual *Pl* assessed from wave parameters derived from SWAN model forced with NCEP/NCAR I reanalysis was 162 $Jm^{-1}s^{-1}$ which represents a very low (and unrealistic) net southward flux. Therefore, three additional global reanalysis (NCEP/DOE II, JRA-25 and ERA-Interim) were implemented to drive SWAN model and, afterward, the corresponding *Pl* were computed.

## *Pl* computed from different global reanalysis

The NCEP/DOE II reanalysis (Kanamitsu et al. 2002) came up with the objective of improving certain aspects of the NCEP/NCAR I reanalysis, extending and updating parameterizations of physical processes. It assimilates the same raw data as NCEP/NCAR I and has the same spatial resolution. JRA-25 (Onogi et al. 2007) is a reanalysis produced by the Japanese Meteorological Agency. Its primary objective is to improve the coverage and quality of atmospheric data in the Asian region. It gives gridded data with a spatial resolution of 1.125° every 6 h. ERA-Interim (Dee et al. 2011) is the most recent reanalysis developed by the European Center for Medium-Range Weather Forecasts (ECMWF). At first, it was conceived as an interim reanalysis in preparation for the next-generation extended reanalysis to replace ERA-40. It uses the ECMWF Integrated Forecast Model and provides data with a spatial resolution of 80 km.

Wave parameters were simulated with SWAN model forced with NCEP/DOE II, JRA-25 and ERA-Interim re-analysis, and net *Pl* were calculated along the coast (Fig. 2). As a result, it can be seen that the highest east-northeastward (negative) *Pl* is obtained when NCEP/NCAR I is used for driving SWAN model, and the highest differences can be appreciated between location 5 and 15. In addition, *Pl* is significantly positive at locations 19 and 20 only when NCEP/NCAR I reanalysis is used as forcing, and *Pl* is practically null when NCEP/DOE II, JRA-25 or ERA-40 are used for driving SWAN model. Finally, the lowest values of *Pl* are obtained when JRA-25 reanalysis is used as forcing.

*Pl* computed from observed wave parameters were compared with *Pl* obtained from simulated parameters using different reanalysis at location 20. Scatter plots for *Pl* computed from observed and simulated parameters for each reanalysis are presented in Fig. 5. The root mean square error ($E_{RMS}$), the

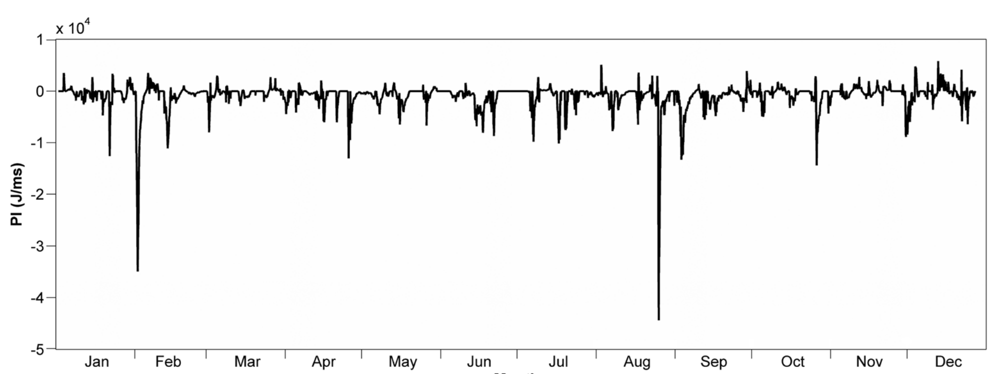


**Fig. 4** Instantaneous *Pl* data series corresponding to the point 20 computed from observed wave parameters at the outer Río de la Plata for 2005. Negative values correspond to northward *Pl*

determination coefficient ($R^2$: the square value of the simple linear correlation coefficient) and the slope of the linear fit ($S_1$) between *Pl* computed from observed and simulated wave parameters for each reanalysis are presented in Table 1. It can be seen that *Pl* obtained from ERA-Interim and JRA-25 reanalysis display similar $R^2$, $E_{RMS}$ and $S_1$. Likewise, NCEP/DOE II and NCEP/NCAR I reanalysis also present similar statistical parameters between them. $R^2$ are significantly different to zero with 95% confidence in all the cases, and the highest $R^2$ are obtained with ERA-Interim and JRA-25. It should be noted that the mean annual *Pl* computed from observed wave parameters was -926 $Jm^{-1}\ s^{-1}$ (significantly northwards) at location 20 (2005), that is, noticeable different to *Pl* computed from different sets of simulated wave parameters (Table 1).

## Discussion

*Pl* computed from simulated wave parameters implementing different reanalysis (2005) provided different values between Bahía Blanca and Punta Médanos (from location 1 to 18, Fig. 2). Although significant differences in magnitude (up to a factor of 6) can be observed between location 5 and 13, the space variability of *Pl* results pretty similar. *Pl* computed from NCEP/NCAR I, NCEP/DOE II, JRA-25 and ERA-Interim present relative maxima and minima at the same locations. Relative maxima are located at sites 4, 7, 10, 14 and 17 and, except for ERA-Interim, the lowest values are located at point 12. Martin et al. (2012) evaluated the performance of NCEP/NCAR I, NCEP/DOE II, JRA-25 and ERA-Interim global databases as atmospheric forcings of SWAN model in the northern Buenos Aires coast. Simulated mean wave heights ranged from 0.63 m (JRA-25) to 0.92 m (NCEP/DOE II). The lowest bias (0.22 m) was obtained when SWAN model was forced with ERA-Interim and the lowest mean square root errors were obtained using NCEP/NCAR I (0.16 m) and NCEP/DOE II (0.19 m). The best slope for simulated heights (0.79) was obtained using NCEP/DOE II. Determination coefficients for heights, periods and directions were very similar (0.89–0.93) for all the simulations. Severe wave events (storms) were specially analyzed. It was shown that the best results during energetic events are achieved using NCEP/DOE II reanalysis. Martin et al. (2012)

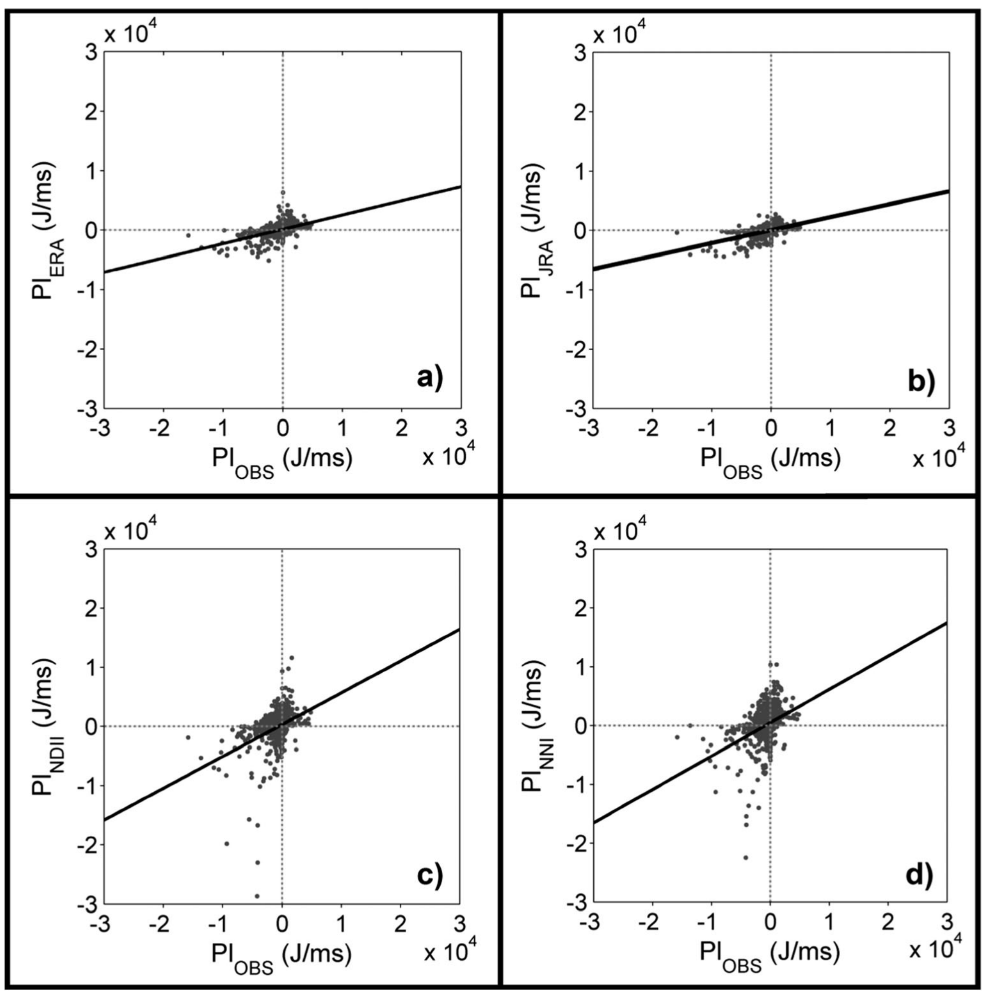


**Fig. 5** Scatter plots for *Pl* computed from observed and simulated parameters simulated with SWAN model, forced with (**a**) ERA-Interim, (**b**) JRA-25, (**c**) NCEP/DOE II and (**d**) NCEP/NCAR I reanalysis

**Table 1** Root mean square error ($E_{RMS}$), determination coefficient ($R^2$: the square value of the simple linear correlation coefficient) and the slope of the linear fit ($S_1$) between *Pl* computed from observed and simulated wave parameters. Net *Pl* computed from simulated wave parameters at location 20, for each reanalysis (2005), are also included

| | $E_{RMS}$ ($Jm^{-1}$ $s^{-1}$) | $R^2$ | $S_1$ | Net *Pl* ($Jm^{-1}$ $s^{-1}$) |
|---|---|---|---|---|
| *ERA-Interim* | 1555 | 0.28 | 0.24 | -3 |
| *JRA-25* | 1519 | 0.31 | 0.22 | −29 |
| *NCEP/NCAR I* | 2315 | 0.16 | 0.56 | 162 |
| *NCEP/DOE II* | 2139 | 0.18 | 0.54 | 10 |

concluded that the best agreement between simulations and observations was obtained using NCEP/NCAR I and NCEP/DOE II as forcing.

It can be easily verified (using eq. 1) that little variations in simulated wave heights using different reanalysis are sufficient to account for significant differences in *Pl*. For example, two simulated wave heights, $H_1 = 0.60$ m and $H_2 = 0.90$ m, give *Pl* that differ in a factor (= $Pl_2/Pl_1$) equal to 2.76 (considering the same wave direction in eq. 1) and, two heights of 0.30 and 0.60 m give a factor equal to 5.66. In addition, very little differences in simulated wave directions would contribute to enlarging the differences when *Pl* is computed using results obtained from different reanalysis. For instance, two simulated wave directions of 3° and 6° give *Pl* values that differ by a factor equal to 1.99 (considering the same wave height in eq. 1). Hence, very little differences in simulated wave heights and directions would explain the dissimilar magnitudes found in *Pl* between location 5 and 18 (Fig. 2). While little differences in wave heights or directions (with $\theta_0$ of the same sign) produce a different intensity of *Pl*, different wave directions (with $\theta_0$ of different sign) produce *Pl* of opposite directions. This would be a possible explanation of why *Pl* presents the same sign but different magnitude between Bahía Blanca and Punta Médanos but opposite sign and very low values between Punta Médanos and Punta Rasa. The predominantly eastward/northward direction of *Pl* between Bahía Blanca and Punta Médanos is supported by the scarce scientific literature. Caviglia et al. (1991) estimated a north-eastward sediment transport rate at Mar del Plata, and Dragani et al. (2013b) estimated a north-northeastward direction of *Pl* at Pinamar, located around 100 km north-eastwards of Mar del Plata. Verón and Bértola (2014) estimated *Pl* from wave parameters computed with WAVEWATCH III model for 2009 in the coast of Buenos Aires and obtained predominantly eastwards/northwards wave energy fluxes with increasing values from Monte Hermoso to Mar del Plata, reaching the highest value at the south of Villa Gesell (Fig. 1), and lower stable values between Pinamar and Punta Rasa.

*Pl* computed from different reanalysis presented dissimilar magnitudes between Bahía Blanca and Punta Médanos (Fig. 1) but, given that its spatial variability is pretty similar, it is possible to carry out a comprehensive analysis of *Pl* throughout the above-mentioned area. Moreover, the following analysis could be seen as independent from the selected atmospheric global data base. First of all, as it was previously highlighted, the direction of *Pl* is definitely eastwards/north-eastwards from location 1 to 18. *Pl* increases from Bahía Blanca to Mar del Plata (Figs. 1 and 2), but this increment is uneven because it increases more significantly from location 4 to 6, 7 to 9 and 10 to 12. Consequently, the potential long shore sediment transport rate (*Q*) would be significantly greater at locations 6, 9 and 12 than at locations 4, 7 and 10, respectively. The long-shore sediment transport budget can be studied in a control volume defined between two transects normal to the coast in the surf zone. The on-shore/off-shore sediment transport is not taken into account in this preliminary analysis. For instance, if a control volume containing locations 4 and 6 is considered, the alongshore sediment budget will be negative and then the coast will be under an important erosive process. These imbalances in the alongshore sediment transport could be a reasonable and preliminary explanation for the reported natural erosion in the southern coast of Buenos Aires (Rojas et al. 2014). On the contrary, *Pl* decreases between Mar del Plata and Punta Médanos, that is, between locations 13 and 19, respectively. But this diminution is not even either (Fig. 2). *Pl* changes appreciably from location 13 to 14 and from 18 to 19. Accordingly, *Q* would be lower at locations 14 and 19 than at locations 13 and 18, respectively. Then, the alongshore sediment budget would become considerably positive, and then the coast would be under a natural constructive process. This fact is observationally supported by means of the survey of systematic beach profiles taken since 2009 between Pinamar and Villa Gesell (Alonso et al. 2015).

Perez et al. (2017) studied the inter-annual variability in *Pl* between Bahía Blanca and Mar del Plata and its relationship with climatic indices related to El Niño/Southern Oscillation (ENSO) and the Southern Annual Oscillation (SAM). Significant correlation coefficients were obtained for both indices which indicated that both climatic anomalies could impact on the wave climate and the littoral processes in the southern coast of Buenos Aires. High interannual variability in *Pl* data series is clearly appreciated in Fig. 3, between Bahía Blanca and Punta Médanos. Even though *Pl* is usually negative (positive) at location 6 (16), positive (negative) values can be observed for years 1983, 1993 and 1998, respectively. In agreement with these anomalous values of *Pl*, the Climate Prediction Center (*http://www.cpc.noaa.gov*) reported ENSO events that occurred in 1982–1983, 1992–1993 and 1997–1998.Consequently, changes in the atmospheric circulation related to the ENSO impacted on the regional wave climate and, as a result, on the littoral processes at the Buenos Aires coast between Bahía Blanca and Punta Médanos. On the other hand, the SAM index (Southern Annual Oscillation, *http://*

www.bom.gov.au/climate/enso/history/ln-2010-12/SAM-what.shtml) which describes the north–south movement of the westerly wind belt, was also considered in order to investigate if anomalous *Pl* computed for 2001 (location 6) could be related to its atmospheric variability. As a result of the present study, anomalous *Pl* computed for 2001 resulted not linked to SAM index.

The northernmost sector of the study region (locations 19 and 20) deserves a particular analysis. In this area, *Pl* is positive (southwards) only when NCEP/NCAR I reanalysis is used as forcing, but it is practically close to zero when NCEP/DOE II, JRA-25 or ERA-40 are used as forcing of SWAN (for 2005). On the contrary, the mean annual *Pl* computed from observed wave parameters for 2005 is -926 $Jm^{-1}$ $s^{-1}$, which corresponds to a net northward flux. Kokot (1997, 2010), based on geomorphological evidence such as the orientation of the sand spit located at Punta Rasa, concluded that the sand must be transported towards the north in this area. Consequently, even though estimating *Pl* from wave parameters (simulated using SWAN model forced by different reanalysis) seems to constitute a very good alternative to study the alongshore wave energy balance from Bahía Blanca to Punta Médanos, this approach does not seem to be a reliable option between Punta Médanos and Punta Rasa. A possible explanation for the significant differences found between *Pl* computed from simulated and observed wave parameters could be some deficiencies in the reanalys is to reproduce wind direction in the northernmost coast of Buenos Aires. Dragani et al. (2008) implemented and validated SWAN model to the Río de la Plata estuary and the adjacent continental shelf using NCEP/NCAR I as atmospheric forcing, and found that monthly *Erms* computed between simulated and observed wave direction could reach up to 80°. Acceptable or little errors in simulated wave directions could significantly distort the directions of *Pl* between Punta Médanos and Punta Rasa, especially, when $\theta_0$ is around zero, that is, when the wave direction is close up to the normal incidence respect to the shoreline. Differences of only a few degrees in simulated wave direction could produce *Pl* with opposite signs when different reanalysis are used as forcing.

## Conclusions

The aim of this paper was to carry out a comprehensive study of *Pl* along the coast of Buenos Aires, between Punta Rasa and Bahía Blanca. *Pl* was estimated from simulated off-shore wave parameters obtained from a validated regional SWAN model, which was forced using NCEP/NCAR I, NCEP/DOE II, ERA-Interim and JRA-25 global reanalysis. Simulated wave parameters provided eastwards/north-eastwards values of *Pl* between Bahía Blanca and Punta Médanos, regardless of the atmospheric forcing (global reanalysis). The spatial variability of *Pl* estimated in each case resulted reasonably similar, differences in magnitude were observed particularly between location 5 and 15. Slight differences in simulated significant wave heights and directions obtained from different forcings could explain the dissimilar magnitudes found in *Pl*. Subsequently, a qualitative analysis of *Pl* was carried out between Bahía Blanca and Punta Médanos. *Pl* definitely flows eastwards/north-eastwards from locations 1 to 18 and increases unevenly from Bahía Blanca to Mar del Plata. Negative imbalances in *Pl* (or *Q*) could be seen as a reasonable and preliminary explanation for the reported natural erosion in the southern coast of Buenos Aires (Rojas et al. 2014). On the contrary, positive imbalances in *Pl* would explain possible constructive process along the coast, which is being evident at Pinamar and Villa Gesell (Fig. 1). High interannual variability was clearly appreciated in *Pl* data series when simulated wave parameters are computed from SWAN model forced by NCEP/NCAR I (period: 1980–2012). It was observed that anomalous *Pl* values detected in the Buenos Aires coast in 1983, 1993 and 1998 are in agreement with reported ENSO events that occurred in 1982–1983, 1992–1993 and 1997–1998. SAM index was also considered in order to investigate whether the anomalous value of *Pl* observed in 2001 could be related to the north–south movement of the westerly wind belt. As a result, this anomalous value of *Pl* for 2001 would not be linked to SAM index. Particular investigations about this subject deserve to be carried out considering other global climatic indices.

The applied methodology seems to be suitable to study the space and time variability of *Pl* along the coast from Bahía Blanca to Punta Médanos (550 km long), but not in the northernmost coast of Buenos Aires, between Punta Médanos and Punta Rasa (67 km long). The implementation of SWAN model including other global reanalysis and regional atmospheric models as forcing is currently being carried out to obtain a better representation of *Pl* in this sector of the coast. It should be highlighted that the lack of systematic observations along the coast of Buenos Aires inflicts a severe constraint to face the study of different coastal processes, many of them very important for coastal management and taking of decisions. Finally, until not to establish a monitoring environmental system in the Buenos Aires coast, the implementation of regional numerical models driven by global reanalysis seems to constitute a suitable methodology which let to deepen the scientific knowledge of many coastal processes along the coast of Buenos Aires.

**Acknowledgments** This paper is a contribution to the CONICET PIP 112-201101-00176 and 112-201501-00174-CO projects.

## References


Alonso G, Dragani WC, Codignotto JO (2015) Impacto del cambio climático en la costa: ¿Se están erosionando las playas del nordeste bonaerense? Proceedings of the IX Jornadas Nacionales de Ciencias del Mar, Ushuaia, Tierra del Fuego, pp 54–55 https://jornadasdelmar2015.files.wordpress.com/2015/11/libro-de-resc3bamenes-final.pdf. Accessed 31 August 2016

Balay M (1955) La determinación del nivel medio del Mar Argentino, influencias de las oscilaciones del mar no causadas por la marea. Servicio de Hidrografía Naval, Armada, p 46

Bayón C, Politis G (1998) Las huellas del pasado: pisadas humanas prehistóricas en la costa pampeana. Ciencia Hoy 8(48):12–20

Booij N, Ris RC, Holthuijsen LH (1999) A third-generation wave model for coastal regions: 1. Model description and validation. J Geophys Res Oceans 104(C4):7649–7666

Caviglia FJ, Pousa JL, Lanfredi NW (1991) A determination of the energy flux constant from dredge records. J Coast Res 7(2):543–549

CERC (1984) Shore Protection Manual. U.S. Army Corps of Engineers, Coastal Engineering Research Center. U.S. Government Printing Office, Washington. D.C., p 640

Codignotto JO, Dragani WC, Martin PB, Simionato CG, Medina RA, Alonso G (2012) Wind-wave climate change and increasing erosion in the outer Río de la Plata, Argentina. Cont Shelf Res 38:110–116

Datawell (1997) Manual for the waverider. In: LM Haarlem. Laboratory for Instrumentation, The Netherlands

Dee DP, Uppala SM, Simmons AJ, Berrisford P, Poli P, Kobayashi S, Andrae U, Balmaseda MA, Balsamo G, Bauer P, Bechtold P (2011) The ERA-interim reanalysis: configuration and performance of the data assimilation system. Q J R Meteorol Soc 137(656):553–597

Dragani WC, Garavento E, Simionato CG, Nuñez MN, Martín P, Campos MI (2008) Wave simulation in the outer Rio de la Plata estuary: evaluation of SWAN model. J Waterw Port Coast Ocean Eng 134(5):299–305

Dragani WC, Martin P, Campos MI, Simionato CG (2010) Are wind wave heights increasing in south-eastern south American continental shelf between 32S and 40S? Cont Shelf Res 30(5):481–490

Dragani WC, Cerne BS, Campetella CM, Possia NE, Campos MI (2013a) Synoptic patterns associated with the highest wind-waves at the mouth of the Río de la Plata estuary. Dyn Atmos Oceans 61-62:1–13

Dragani WC, Martin PB, Alonso G, Codignotto JO, Prario BE, Bacino G (2013b) Wind wave climate change: impacts on the littoral processes at the northern Buenos Aires Province coast, Argentina. Clim Chang 121(4):649–660

Fiore MME, D'Onofrio EE, Pousa JL, Schnack EJ, Bértola GR (2009) Storm surges and coastal impacts at Mar del Plata, Argentina. Cont Shelf Res 29(14):1643–1649

Galvin CJ, Schweppe CR (1980) The SPM Energy Flux Method for Predicting Longshore Transport Rate. Coastal Engineering Research Center, Fort Belvoir Va, Technical Paper No. 80–4

Isla FI (2015) Spatial and temporal variations of the Litoral drift, southeastern Buenos Aires Province, Argentina. Revista Geográfica del Sur 5(8):24–41

Juárez VI, Mantobani JM (2006) La costa bonaerense: un territorio particular. In: Isla FI, Lasta CA (eds) Manual de manejo costero para la provincia de Buenos Aires. EUDEM, pp 41–71

Kalnay E, Kanamitsu M, Kistler R, Collins W, Deaven D, Gandin L, Iredell M, Saha S, White G, Woollen J, Zhu Y (1996) The NCEP/NCAR 40-year reanalysis project. Bull Am Meteorol Soc 77(3):437–471

Kanamitsu M, Ebisuzaki W, Woollen J, Shi-Keng Y (2002) NCEP-DOEAMIP-II reanalysis (r-2). Bull Am Meteorol Soc 83(11):1631–1644

Kokot RR (1997) Littoral drift, evolution and management in Punta Médanos, Argentina. J Coast Res 13(1):192–197

Kokot RR (2010) Espigas indicadoras de proveniencia de olas en la costa argentina. Rev Asoc Geol Argent 67(1):19–26

Lanfredi NW, Pousa JL, Mazio CA, Dragani WC (1992) Wave-power potential along the coast of the province of Buenos Aires, Argentina. Energy 17(11):997–1006

Marcomini SC, López R (2006) Geomorfología costera y explotación de arena de la playa en la provincia de Buenos Aires y sus consecuencias ambientales. Rev Bras Geomorf 7(2):61–71

Martin P, Dragani WC, Cerne B, Alonso G, Pescio A, Prario B (2012) Numerical simulation of wind waves on the Río de la Plata: evaluation of four global atmospheric databases. Braz J Oceanogr 60(4):501–511

Merlotto A, Bértola G, Isla F, Cortizo L, Piccolo M (2013) Short and medium-term coastal evolution of Necochea municipality, Buenos Aires province, Argentina. Environ Earth Sci 71:1213–1225

Onogi K, Tsutsui J, Koide H, Sakamoto M, Kobayashi S, Hatsushika H, Matsumoto T, Yamazaki N, Kamahori H, Takahashi K, Kadokura S (2007) The JRA-25 reanalysis. J Meteorol Soc Jpn 85(3):369–432

Perez I, Alonso G, Pescio AE, Dragani WC, Codignotto JO (2017) Longshore wave energy flux: variability and trends in the southern coast of Buenos Aires, Argentina. Reg Stud Mar Sci 16:116–123

Quefeffeulou P, Croizé-Fillon D (2013) Global altimeter SWH data set - May 2013. Plouzané, Francia: Laboratoire d'Océanographie Spatiale, IFREMER

Rojas ML, Recalde MY, London S, Perillo GM, Zilio MI, Piccolo MC (2014) Behind the increasing erosion problem: the role of local institutions and social capital on coastal management in Argentina. Ocean Coast Manag 93:76–87

SHN (1986) Mar Argentino, de Río de la Plata al Cabo de Hornos. Carta Náutica 50, 4th edn. Servicio de Hidrografía Naval, Buenos Aires

SHN (1992) Acceso al Río de la Plata. Carta Náutica H1, 5th edn. Servicio de Hidrografía Naval, Buenos Aires

SHN (1999a) Río de la Plata Medio y Superior. Carta Náutica H116, 4th edn. Servicio de Hidrografía Naval, Buenos Aires

SHN (1999b) Río de la Plata Exterior. Carta Náutica H113, 2nd edn. Servicio de Hidrografía Naval, Buenos Aires

SHN (2017) Tablas de Marea. Ministerio de Defensa. Servicio de Hidrografía Naval, Buenos Aires

Simionato CG, Vera CS, Siegismund F (2005) Surface wind variability on seasonal and interannual scales over Río de la Plata area. J Coast Res 21(4):770–783

Simionato CG, Meccia VL, Dragani WC, Nuñez MN (2006a) On the use of the NCEP/NCAR surface winds for modeling barotropic circulation in the Río de la Plata estuary. Estuar Coast Shelf Sci 70(1):195–206

Simionato CG, Meccia VL, Dragani WC, Guerrero R, Nuñez MN (2006b) Río de la Plata estuary response to wind variability in synoptic to intraseasonal scales: Barotropic response. J Geophys Res: Oceans, 111(C9)

Simionato CG, Meccia VL, Guerrero R, Dragani WC, Nuñez MN (2007) Rio de la Plata estuary response to wind variability in synoptic to intraseasonal scales: 2. Currents' vertical structure and its implications for the salt wedge structure. J Geophys Res Oceans 112(C7)

Simmonds I, Keay K (2000) Mean southern hemisphere extratropical cyclone behavior in the 40-year NCEP-NCAR reanalysis. J Clim 13(5):873–885

U.S. Army Corps of Engineers (2017) Coastal engineering manual. Engineer manual 1110–2-1100, U.S. Army Corps of Engineers, Washington, D.C., p 2156

Verón MJ, Bértola GR (2014) Aplicación del método de flujo de energía en el litoral de la provincia de Buenos Aires, Argentina. Lat Am J Sedimentol Basin Anal 21(1):17–23